**Title**

# Evolution of the ribbon-like organization of the Golgi apparatus in animal cells

**Authors**

Giovanna Benvenuto[1§], Serena Leone[1§], Emanuele Astoricchio[1], Sophia Bormke[2], Sanja Jasek[3], Enrico D'Aniello[1], Maike Kittelmann[4], Kent McDonald[5], Volker Hartenstein[6], Valentina Baena[7], Héctor Escrivà[8], Stephanie Bertrand[8], Bernd Schierwater[9], Pawel Burkhardt[10], Iñaki Ruiz-Trillo[11], Gáspár Jékely[3], Jack Ullrich-Lüter[2], Carsten Lüter[2], Salvatore D'Aniello[1], Maria Ina Arnone[1], Francesco Ferraro[1,12,*]

**Authors affiliations**

[1]Department of Biology and Evolution of Marine Organisms, Stazione Zoologica Anton Dohrn (SZN), Naples, Italy; [2]Museum für Naturkunde, Berlin, Germany; [3]Living Systems Institute, University of Exeter, Exeter, UK; [4]Department of Biological and Medical Sciences, Oxford Brookes University, Oxford, UK; [5]Electron Microscope Lab, University of California Berkeley, Berkeley, CA, U.S.A; [6]Department of Molecular, Cell and Developmental Biology, University of California Los Angeles (UCLA), Los Angeles, CA, U.S.A.; [7]Department of Cell Biology, UConn Health, Farmington, CT, U.S.A.; [8]Sorbonne Université, CNRS, Biologie Intégrative des Organismes Marins, BIOM, F-66650, Banyuls-sur-Mer, France; [9]Institute of Ecology and Evolution, Hannover University of Veterinary Medicine Foundation, Hannover, Germany; [10]Michael Sars Centre, University of Bergen, Bergen, Norway;[11]Institut de Biologia Evolutiva (CSIC-Universitat Pompeu Fabra), Barcelona, Spain.

[§] These authors contributed equally

* Correspondence: francesco.ferraro@szn.it

[12]Lead contact

**Keywords**

Golgi structure; Golgi ribbon; organelle; evolution; metazoans; GRASP, Golgin-45; AlphaFold2; development.

**Summary**

The Golgi ribbon is a structural organization formed by linked Golgi stacks that is believed to be exclusive to vertebrate cells. Its functional contribution to cellular processes is unclear, yet its disruption is associated with several human pathologies. In this study we address the evolutionary origin of the Golgi ribbon, describe a potential molecular mechanism for its emergence and identify a cellular process in which it may be involved. We observed the ribbon-like architecture in the cells of several metazoan taxa, suggesting its early appearance during animal evolution before the emergence of vertebrates. Supported by AlphaFold2 modelling, we propose that the evolution of the complex between two Golgi resident proteins, Golgin-45 and GRASP, led to the tethering of Golgi stacks into the ribbon-like configuration. Finally, we find that the ribbon is assembled during the early embryogenesis of deuterostome animals, a strong indication of its role in development. Overall, our study indicates that the Golgi ribbon is functionally relevant beyond vertebrates and calls for further investigations to decipher its elusive functions.

## Introduction

Sitting at the center of the exocytic pathway, the Golgi apparatus is involved in the processing and sorting of secretory cargoes. This biosynthetic function remains the most actively investigated[1-3], but recent evidence indicate that the Golgi is also involved in secretion-independent cellular processes, such as stress sensing and signaling, apoptosis, autophagy, proteostasis and innate immunity[4-11]. The Golgi's fundamental structural unit is the stack, formed by a pile of flat membrane saccules, known as cisternae. Across eukaryotes, the Golgi occurs as a single- or multi-copy organelle, depending on the number of stacks per cell. In animals, when present as multi-copy organelle, the Golgi is observed in two configurations: stacks either remain separate or link to each other into a single centralized structure that was first described as "ribbon-like" by Camillo Golgi[12]. The current consensus is that the Golgi ribbon is present only in vertebrate cells. Despite having been widely investigated, for the most part in cultured mammalian cells, the biological functions of the Golgi ribbon still remain obscure[13-15] and it is unclear which selective pressures might have led to the evolution of this Golgi configuration. During mitosis, mammalian cells disassemble and reassemble the ribbon in a finely tuned process[16]; such a level of regulation suggests that the ribbon architecture must be functionally important. This conclusion is supported by the existence of several pathologies in which ribbon breakdown (Golgi "fragmentation") is a morphological phenotype, most notably neurodegenerative diseases but also cancer and viral infections[17-23]. Therefore, deciphering the roles that the Golgi ribbon plays in cellular physiology may also help us understand the pathological consequences stemming from its disruption.

In this study, through a comparative approach borrowed from evolutionary studies, we asked three questions regarding the ribbon architecture of the Golgi apparatus. 1) When did it appear during animal evolution? 2) Which molecules might have mediated this structural innovation? 3) Which biological functions does it carry out? We answer the first one; propose a testable hypothesis for the second one; and, regarding the third one, we produce experimental data that point toward development as a biological process in which the ribbon may play a functional role.

## Results

### A ribbon-like Golgi complex is common in animals

According to the current consensus, only vertebrate cells form Golgi ribbons. Therefore, we were intrigued by morphological data showing Golgi centralization in the embryos of two sea urchin species, *Strongylocentrotus purpuratus* and *Lytechinus variegatus*[24,25], hinting at the possibility that the ribbon organization of the Golgi might be more common than thought at present. To assess if this is the case, we surveyed the Golgi ultrastructure in representatives of several animal taxa and closely related unicellular eukaryotes, which, together, comprise the eukaryotic holozoan clade. We had to distinguish between *bona fide* ribbon and ribbon-like architectures. In mammalian cells the Golgi ribbon is characterized by some level of membrane continuity between cisternae of adjacent stacks, which can be detected by fluorescent recovery after photobleaching assays and electron tomography[26,27]. As our survey relied for the most part on electron micrographs of thin sections where membrane continuity between cisternae of juxtaposed stacks cannot be easily assessed, we describe Golgi organizations reminiscent of the mammalian ribbon as ribbon-like. Golgi stack dimers have been observed in *Drosophila melanogaster* cells[28], which have dispersed Golgi elements[29], and even in mammalian cells after ribbon unlinking by microtubule depolymerization[30]. Therefore, we identified Golgi complexes as “ribbon-like” only when three or more closely apposed stacks were observed in electron micrographs (Figure 1A). In mammalian cell types, the ribbon architecture, though common, is not ubiquitous. Differentiated tissues such as muscles, acid-secreting gastric cells, and spinal ganglion neurons, for instance, display Golgi complexes made by separated stacks[31-33]. For this reason, wherever possible, several cell types of the organisms under consideration were inspected and, whenever available, we supplemented our survey with morphological evidence from the literature.

We first looked at bilaterians. In the cells of the marine worm *Symsagittifera roscoffensis* (xenacoelomorph), separated stacks were observed (not shown). Interestingly, some of its secretory cells displayed closely apposed, though clearly distinct, Golgi stacks: an intermediate organization between separated Golgi elements and a ribbon-like organization (Figures 1B and S1A). Ribbon-like Golgis were found in epidermal cells of the three-lobed larva of the brachiopod *Calloria inconspicua* and in several cell types of the marine annelid *Platynereis dumerilii* (Figures 1C, 1D, S1B and Movie S1). As Ramón y Cajal described ribbon-like Golgis in neurons and epithelial cells of the common earthworm[34], we conclude that this

Golgi organization is common among annelids. In mollusks, a centralized Golgi that fragments at mitosis was observed in spermatocytes of the snail *Paludina vivipara* more than a century ago[35], while other reports show ribbon-like Golgi complexes in other species (e.g., *Helix pomatia*[36] and *Helix aspersa*[37]). Cells of the roundworm *Caenorhabditis elegans*, a nematode, and of the fruit fly *Drosophila melanogaster*, an arthropod, two model organisms widely used in genetics and cell biology, display Golgi complexes consisting of several, separated stacks[28,29,38,39]. To test whether Golgi stack decentralization is an arthropod feature, as opposed to *Drosophila*/insect-specific, we analyzed the ultrastructure of the crustacean *Parhyale hawaiensis*, observing separated stacks in neurons (Figure 1E) and in all other inspected cell types (not shown). It is therefore likely that a decentralized Golgi is the typical configuration in arthropods, not just of *Drosophila* and other insects (e.g., bees, aphids, and mosquitos[40-42]). We then analyzed cnidarians: in the hydrozoan *Clytia hemisphaerica*, the secretory gland cells of the gastroderm, but not other cell types, display stacks linked into a ribbon-like structure (Figure 1F), which is also observed in phagocytic cells of another cnidarian, the actinia *Phelliactis robusta*[43]. In the ctenophore *Mnemiopsis leidyi*, epithelial and comb cells (Figures 1G and S1C), nerve net neurons, mesogleal neurons, and sensory cells[44,45] all display separated stacks. Among other animals, we found a single Golgi stack in all cells of two placozoan species: *Trichoplax adhaerens* (Figures 1H, S1D and S1E) and *Hoilungia hongkongensis*[46]. Like placozoans, the sea sponge *Oscarella carmela* (Figure 1I and reference[47]) and other species (genera *Chondrosia*, *Crambe* and *Petrosia*; not shown) have a single Golgi stack per cell. In choanoflagellates and filastereans, which are unicellular holozoans, the Golgi is also present as a single stack per cell (Figure 1J and references[47,48]).

Vertebrates (chordates) and echinoderms (ambulacraria) belong to the deuterostome clade of bilaterian animals. We assessed whether the Golgi ribbon is found in non-vertebrate deuterostomes, investigating the ultrastructure of a sea urchin, a tunicate and a cephalochordate species. Indeed, we find that all three species display ribbon-like Golgis (see section “Developmental assembly of the Golgi ribbon”, below).

In summary, despite a relatively small sampling (Figure S1F), ribbon-like Golgi complexes are easily observed in cells of cnidarians and bilaterians, and not found outside these animal taxa. Obviously, the presence of multiple stacks per cell is a

precondition for their clustering and ribbon formation, but it appears to be not sufficient. Point in case are sponges, which usually display a single Golgi stack per cell (Figure 1I and reference[47]); however, in rare instances, such as the gemmule's spongocytes of the freshwater species *Ephydatia fluviatilis*[49], sponge cells with multiple stacks are observed, but remain separate. It should be noted that in our survey, except for *Platynereis dumerilii* and *Strongylocentrotus purpuratus* (Figure S1B, Movie S1 and Figure S4E) for which volume electron microscopy was available, the thin section electron micrographs did not allow to assess whether all the Golgi stacks in a cell are linked into a single ribbon-like organization or form multiple "mini-ribbons". Nonetheless, in those cases where we identified a ribbon-like organization we can state that the process of stack centralization is clearly observed. In conclusion, the most parsimonious explanation accounting for our results and the literature's data is that the ribbon-like Golgi likely evolved in the common ancestor of cnidarians and bilaterians, and was secondarily lost in xenacoelomorphs, arthropods, and nematodes (Figure 1K).

**Putative molecular mediators of ribbon-like Golgi emergence**

Next, we asked which molecular innovations might have driven the emergence of the ribbon-like Golgi organization. If, as our survey suggests, this was a single evolutionary event, conservation of the molecular mechanisms of its formation would be expected. Among the several factors involved in the formation of the mammalian Golgi ribbon[50], the molecular tethers GRASP (Golgi Reassembly and Stacking Protein) and the coiled-coil proteins collectively known as Golgins play a central role (Figure 2A)[50-56]. GRASPs comprise an evolutionarily conserved GRASP region, made of two atypical PDZ domains in tandem, and a more variable C-terminal unstructured region (Figures S2A and S2B). While GRASPs are encoded by a single gene in most eukaryotes, a duplication gave rise to two paralogs in jawed vertebrates (Figure S2C Data S1). Involved in several cellular processes[57-60], GRASPs are capable of self-interaction and while they were initially considered to promote cisternal adhesion within the stack[61-63], recent work unequivocally showed that they mediate Golgi stack tethering and ribbon formation but not cisternal stacking[55,56]. The two mammalian paralogs, GRASP55 and GRASP65, are recruited to Golgi membranes by myristoylation of the glycine in position 2[61,64], which is conserved across holozoans (Data S1), and by interaction with Golgin-45 and

GM130, respectively (Figure 2A)[65,66]. Such dual-anchoring is required for ribbon formation as it spatially orients GRASPs and allows their homo-dimerization/oligomerization in *trans*, thus tethering membranes of distinct Golgi stacks and promoting ribbon formation[67-69]. Golgins mediate vesicular traffic specificity[70-72] and their knockdown results in secretory defects and ribbon unlinking into constituent stacks[50,53]; though, it is not clear whether these two phenotypes depend on the same or separate functions that Golgins play. The *Golgin-45* gene is an innovation of holozoan eukaryotes[73]. In mammals, the Golgin-45 protein interacts with the GRASP paralog GRASP55 (Figure 2A)[66]; and in cultured cells, either Golgin-45 knockdown or long-term degron-induced ablation of GRASP55, but not of GRASP65, result in Golgi ribbon unlinking[56,66]. As GRASP55 is more similar to the single GRASP proteins present in non-vertebrate bilaterians and cnidarians (Figure S2C), it is plausible that evolution of GRASP binding by Golgin-45 may have led to GRASP-mediated stack tethering (i.e., centralization) and ribbon-like Golgi evolution (Figure 2B). We searched and identified the Golgin-45 homologs in representatives of metazoans and of their closer unicellular relatives, confirming previous findings that this protein evolved in the common ancestor of holozoans[73]. In addition, we found that the *Golgin-45* gene was lost in choanoflagellates, and, among metazoans, in most xenacoelomorphs (Data S2), which interestingly do not display ribbon-like Golgi (Figures 1B and S1A).

The crystal structure of the complex between the C-terminus of mouse Golgin-45 and the GRASP domain of the conspecific GRASP55 has been solved[74], highlighting the existence of three main interaction sites between the two proteins: i) a PDZ-binding motif spanning the four C-terminal amino acids of Golgin-45; ii) an atypical Zinc finger composed by two cysteines of Golgin-45 and a cysteine and a histidine in the GRASP domain; iii) the insertion of nine residues of Golgin-45 into the hydrophobic groove between the two PDZ domains of GRASP55 (Figure S2D)[74]. Binding experiments showed that the PDZ-binding motif and the cysteine pair are necessary for Golgin-45/GRASP complex formation, whereas the contribution of the groove-interacting residues remains unclear[74] (Supplemental Results and Discussion). We aligned the C-terminal sequences of holozoan Golgin-45 proteins to assess conservation of the amino acids involved in GRASP interaction (Figure S2E). The PDZ binding motif and the cysteine pair are highly conserved, with the notable exception of *Drosophila melanogaster* and *Parhyale hawaiensis*, whose cells lack

ribbon-like Golgi organization (Figure S2E, refs.[28,29] and Figure 1E), whereas the Golgin-45 residues corresponding to those that interact with the GRASP groove are more variable across holozoans (Figure S2E).

As the untemplated AlphaFold2 model[75,76] of the mouse Golgin-45/GRASP complex was generated with high confidence and was very similar to the crystal structure (Figure 2C and Supplemental Results and Discussion), we reasoned that Golgin-45/GRASP interactions may be predicted[77,78] by modelling complexes of conspecific protein pairs. We considered binding to occur when GRASP interaction with the PDZ-binding motif and formation of the Zinc finger could be detected in the modelled complex. In bilaterians and cnidarians, all models predicted binding, except for arthropods (*Drosophila melanogaster* and *Parhyale hawaiensis*), nematodes (*Caenorhabditis elegans*) and the only xenacoelomorph species in which the *Golgin-45* gene is still present, *Hofstenia miamia* (Figures 2D and S3A). Golgin-45 was not predicted to bind its conspecific GRASP in ctenophores, porifera and unicellular filastereans (Figure 2D). The reliability of AlphaFold2 predictions was corroborated by modeling the complexes of various point mutants of the mouse Golgin-45 PDZ-binding motif, cysteine pair, and groove interacting residues that had been experimentally tested in *in vitro* GRASP binding assays[74]. The models obtained were consistent with the experimental data by those authors (Figure S3B and Supplemental Results and Discussion). We therefore deduce that a stable Golgin-45/GRASP interaction is present in cnidarians and bilaterians, likely appearing in their common ancestor, but was impaired by subsequent amino acid mutations in the Golgin-45 proteins of arthropods, nematodes, and in the only extant one of xenacoelomorphs (Figure S3A). In conclusion, AlphaFold2 models lend support to our hypothesis that the evolution of GRASP binding by Golgin-45 may have driven the appearance of stack tethering and the emergence of the ribbon-like Golgi organization (Figure 2E).

**Developmental assembly of the Golgi ribbon**

As published morphological data were indicative of Golgi centralization in sea urchins[24,25], we analyzed Golgi dynamics in the embryo of the sea urchin species *Paracentrotus lividus*. Time-course analysis of a fluorescent Golgi reporter showed that early in development, throughout the cleavage stage, the Golgi is present as separate elements which then cluster into centralized structures before hatching of

the blastula (Figures 3A, S4A and S4B). Golgi clustering is rapid: within one hour, Golgi elements increase 10-fold in size while their number decreases 3-fold (Figures 3B, 3C and Movie S2). Afterwards, centralized Golgi complexes are observed in all cells of the embryo and at all developmental stages up to the planktonic pluteus larva (Figures 3A and S4C) and confocal imaging at higher magnification of post-clustering stages showed a morphology strongly reminiscent of the Golgi ribbon as observed in mammalian cells (Figure S4D). At the ultrastructural level, the arrangement of the sea urchin Golgi elements recapitulated confocal microscopy observations. Separated stacks cluster and finally establish connections with each other during early development, confirming that sea urchins centralize their Golgi apparatus into a ribbon-like architecture (Figure 3D). Centralized Golgi complexes were previously observed in the gastrula and prism stages of *Strongylocentrotus purpuratus*[24]. Indeed, we also observed ribbon-like Golgi complexes in the pluteus larva of this sea urchin species (Figure S4E). Like the ribbon of mammalian cells, sea urchin's centralized Golgi undergoes disassembly/reassembly cycles during mitosis (Figure S4F) and its maintenance requires an intact microtubule network (Figures S4G and S4H)[14,16,79-81]. All these characteristics strongly indicate that the centralized Golgi complexes of sea urchin cells are *bona fide* ribbons. As echinoderm representatives, sea urchins form part of the sister group to all chordates, including vertebrates. Therefore, the mechanisms mediating formation of the Golgi ribbon and its developmental timing might be conserved across the deuterostome clade. Indeed, we observed developmental Golgi stack clustering and ribbon-like formation in the cells of two non-vertebrate chordates, the sea squirt *Ciona robusta* (tunicate) and the lancelet *Branchiostoma lanceolatum* (cephalochordate) (Figures 3E and 3F). Golgi centralization also occurs in mouse embryos during the preimplantation stage[82], indicating that the developmental ribbon assembly is indeed a conserved feature across deuterostomes. Such a Golgi dynamics suggests that the developmental switch from separated Golgi stacks to the ribbon-like configuration might play an important role during the initial stages of embryogenesis.

## Discussion

While the functions played by the ribbon remain unaddressed, indirect evidence suggest that this Golgi configuration must play important functions in cellular

physiology. Firstly, the mammalian ribbon disassembles and reassembles during mitosis in proliferating cells; this process involves a finely timed regulation[16], which is unlikely to have evolved to support the inheritance of a cellular structure with no biological role. Secondly, Golgi "fragmentation", meaning ribbon disruption, is a morphological phenotype of several human pathologies, among which most notable are neurodegenerative diseases. For instance, in animal models of Amyotrophic Lateral Sclerosis (ALS), Golgi fragmentation precedes phenotypic manifestations[17]. In cellular models of Alzheimer's, Golgi fragmentation promotes Aβ peptide production[19], and, in glutamatergic neurons differentiated from induced pluripotent stem cells that carry familial Alzheimer's disease mutations, Golgi fragmentation is one of the earliest morphological phenotypes detected[23]. From this body of observations, it follows that deciphering which biological functions the Golgi ribbon carries out would not only advance our knowledge of cellular physiology but also help us to better understand the pathological implications of the disruption of this structure. By adopting a comparative perspective that places Golgi architecture in an evolutionary context, here we outline the origins of the ribbon-like organization, propose which molecular effectors may have been responsible for its emergence, and identify its developmentally regulated formation that may signal its function in embryogenesis.

Previously to the present study, the ribbon organization of the Golgi apparatus was thought to be unique to vertebrates. The lack of a centralized Golgi in the cells of *D. melanogaster* and *C. elegans*, two invertebrates widely used in cell biology, may have contributed to cement this view. Nonetheless, works dating to the early 1900's already showed the presence of ribbon-like Golgi complexes in non-vertebrates[34,35], and further evidence from electron microscopy analyses of various animal cells accumulated later[36,37,43,83]. Building on this body of literature we sampled species representative of diverse metazoan taxa and show that ribbon-like centralization of Golgi stacks is likely to be a newly evolved character of the ancestor of cnidarians and bilaterians. The frequency with which ribbon-like Golgi complexes are found, both in our morphological analyses and in the literature, supports the generalizations we made on its evolutionary emergence and secondary loss at the level of phyla and superphyla (Figure 1K). Evolutionary conservation of the ribbon-like Golgi configuration in several animal phyla strongly indicates that it must play important

functions in their cellular processes. It also begs the question of how did the cells of xenacoelomorphs and ecdysozoans adapt to its secondary loss. Comparative analysis of cellular processes between animals which conserved the ribbon-like Golgi and those which lost it may provide clues regarding the functions this structure is involved in.

Based on experimental evidence from mammalian cells, we propose a plausible molecular mechanism for the appearance of the ribbon-like Golgi organization. GRASP "resurrection" experiments indicate that the self-interacting capability of this protein is ancestral[84]. Bootstrapping on this function, and in the context of cells with multiple Golgi stacks, evolution of GRASP binding by Golgin-45 may have driven ribbon-like emergence in the ancestor of cnidarians/bilaterians. This hypothesis invokes a central role for Golgin-45/GRASP interaction in the evolution and conservation of the mechanism of formation of Golgi ribbons. We focused on Golgin-45 as in mammals it interacts with GRASP55, which is the paralog more similar to the only GRASP present in cnidarians and non-vertebrate bilaterians (Figure S2C). Sequence variations in protein homologs represent natural experiments in mutagenesis. Taking advantage of such experiments done by evolution, we used AlphaFold2 to predict Golgin-45/GRASP binding across holozoans. The results provide support to our hypothesis as they concur with our morphological observations regarding the presence of a ribbon-like Golgi in extant metazoans (Figures 1K and 2E). Whether conspecific Golgin-45 and GRASP proteins do or do not interact as predicted by AlphaFold2 remains to be experimentally tested. It also needs to be established through experiment whether the linked Golgi stacks documented in cnidarians/bilaterians reflect the presence of *bona fide* ribbons; in other words, whether the Golgin-45-dependent spatial orientation of GRASP on Golgi membranes is conducive not only to stack tethering but also to membrane continuity between cisternae of juxtaposed stacks, as observed in mammalian cells[26,27,85]. Mammalian GRASPs are necessary for ribbon formation and GRASP55 interacts with tens of proteins[56,86]. Therefore, it is possible that, by recruiting a network of interactors, oligomerization of correctly oriented GRASP could provide a multivalent molecular platform that directly mediates Golgi stack tethering, and indirectly coordinates the activity of several factors in the formation and maintenance of the Golgi ribbon. Our Golgin-45/GRASP binding hypothesis can be tested in its

aforementioned declinations through a comparative approach that takes advantage of the recent addition to lab experimentation of several non-vertebrate animal, such as the cnidarians *Clytia hemisphaerica* and *Nematostella vectensis* or the annelid *Platynereis dumerilii* [87-89], and of other established vertebrates and invertebrate experimental organisms.

In eukaryotes, complex multicellularity evolved several times[90], but non-animal multicellular organisms, such as plants and fungi, display multiple separated Golgi stacks[91-93]. Golgi centralization may thus indicate an evolutionary trajectory with functional requirements specific to cnidarians/bilaterians and divergent from those of basal animals and other multicellular organisms. In this evolutionary context, the question thus arises as to which functions did the ribbon-like Golgi organization evolve to carry out. Were the ribbon, as believed until now, a Golgi configuration restricted to vertebrates, then its functions could have been struck off as specific to this animal lineage. Our findings imply otherwise; at least some of the biological processes the ribbon-like Golgi attends to must be common to all cnidarians/bilaterians. The observation that the ribbon is formed early in embryogenesis (this report and reference[82]) may indicate that, in the context of the whole organism, its first function is linked to development, which would explain why some differentiated mammalian tissues can forgo Golgi ribbons[31-33]. From an evolutionary point of view, it is intriguing to speculate that this may also have been the primordial function of the ribbon-like Golgi. In this hypothetical scenario, the developmental processes of xenacoelomorphs, arthropods and nematodes must have adapted to dispense with the ribbon-like Golgi altogether.

In conclusion, the main finding of the present study is that ribbon centralization into a ribbon-like configuration is common to several animal taxa with well-developed cell types. By the principle of parsimony, we assume that such a situation is explained by a single evolutionary event occurring in the common ancestor of these animals. We expect our report to spark renewed interest in the ribbon configuration of the Golgi apparatus with new studies aimed at testing our hypotheses on its molecular origins and its function in the context of development.

**Acknowledgements**

We thank Laura Núñez Pons, Filomena Ristoratore, and Periklis Paganos (Stazione Zoologica Anton Dohrn, SZN, Naples, Italy) for providing electron micrographs of sea sponges, of the sea urchin *Strongylocentrotus purpuratus* and helping with the anatomy of the *Ciona intestinalis* larva; Evelyn Houliston (Laboratoire de Biologie du Développement de Villefranche-sur-mer, France) and Mark Terasaki (UConn Health, Farmington, CT, USA) for providing the *Clytia hemisphaerica* electron micrograph; Elisabeth Knust and Michaela Yuan (Max-Planck-Institute of Molecular Cell Biology and Genetics, Dresden, Germany) and Xavier Bailly (Centre National de la Recherche Scientifique & Université Pierre et Marie Curie, CNRS-PMC, Roscoff, France) for their help with *S. roscoffensis* samples; Pedro Martinez Serra (Departament de Genetica, Microbiologia i Estadística, Universitat de Barcelona, Spain) for his valuable suggestions; Martin Lowe (School of Biological Sciences, Division of Molecular & Cellular Function, University of Manchester, UK) and Evelyn Houliston (Laboratoire de Biologie du Développement de Villefranche-sur-mer, France) for their comments on the manuscript. Francesco Ferraro is supported by SZN intramural funding. Emanuele Astoricchio is supported by a PhD fellowship funded by the Stazione Zoologica Anton Dohrn (Open University – Stazione Zoologica Anton Dohrn PhD Program).

**Author contributions**

Conceptualization: F.F. Methodology: F.F., M.I.A., S.D., S.L. Investigation: F.F., G.B., S.L., E.A., S.Bo. Resources: S.J., M.K., K.M., V.H., V.B., H.E., S.Be., C.L., J.U-L., B.S., P.B., I.R-T., G.J., E.D. Writing original draft: F.F. Review & Editing: F.F., G.B., S.L., H.E., S.Be, S.D, J.U-L., C.L., I.R-T., B.S., G.J., P.B., M.I.A.. Visualization: F.F. Supervision: F.F.

**Declaration of interests**

The authors declare no competing interests.

**Inclusion and diversity statement**

The authors support inclusive, diverse, and equitable conduct of research.

**Figure titles and legends**

**Figure 1. Golgi architecture in holozoans.** The Golgi organization in holozoan exemplars from diverse taxa was analyzed at the ultrastructural level; separated and linked stacks are highlighted in light ochre and light magenta, respectively. (A) Observation of three or more Golgi stacks in close contact and/or with membrane continuities is the criterion adopted for positive identification of the ribbon-like configuration in electron micrographs. (B) The xenacoelomorph *Symsagittifera roscoffensis* (Roscoff worm), secretory cell. (C) The brachiopod *Calloria inconspicua*, epidermal cell of the mantle lobe of the three-lobed larva. (D) The annelid *Platynereis dumerilii*, glial cell of the 3-day old larva. (E) The crustacean *Parhyale hawaiensis*, nerve cell. (F) The cnidarian *Clytia hemisphaerica*, gonad gastrodermal cells. (G) The ctenophore *Mnemiopsis leydi*, epithelial cells. (H) The placozoan *Tricoplax adhaerens*. (I) The sea sponge *Oscarella carmela*, choanocyte. (J) The filasterean *Capsaspora owczarzaki.* Scale bars: 1 µm. (K) Deduced evolutionary emergence of the ribbon-like Golgi organization. Ribbon-like absence in both arthropods and nematodes, which both belong to the ecdysozoan superphylum, may indicate that loss of Golgi stack linking occurred in their common ancestor. See also Figure S1 and Movie S1.

**Figure 2. Putative molecular mediators of the ribbon-like Golgi emergence.** (A) The Golgi localized molecular tethers Golgins and GRASPs. Golgins are coiled-coil proteins that localize to Golgi membranes by a transmembrane region or through recruitment by small GTPases of the Rab, Arl and Arf families. Golgin localization within the stack (see references[50,52,53,94,95]), their sizes (human homologs, bar length), and their evolutionary emergence[73] are indicated. (B) Evolution of GRASP-mediated Golgi stack tethering. In mammalian cells, dual anchoring of GRASPs on Golgi membranes is required for self-interaction in *trans* and stack tethering. GRASP myristoylation is ancestral (see text and Data S1) and therefore its dual anchoring to Golgi membrane should originate from the evolution of binding by Golgin-45, leading to the emergence of stack linking and ribbon formation. (C) Solved structure (X-ray; PDB accession code 5H3J) and the AlphaFold2 (AF2) model of the mouse Golgin-45/GRASP complex. AF2 predicted structure almost overlaps the experimentally solved one (RMSD 3.040 Å for the Cα of the last 16 amino acids of the Golgin-45 C-terminal peptide). (D) AF2 models of holozoan GRASPs in complex with their conspecific Golgin-45 C-termini. Altered conformations, with respect to the mouse

complex, are indicated by the arrows (blue for the PDZ-binding motif, red for the cysteine pair and green for the GRASP groove-interacting residues). (E) Presence and inferred evolutionary origin of GRASP binding by the C-terminus of Golgin-45, as deduced by AlphaFold2 modelling of complexes. See also Figures S2 and S3, Data S1 and S2.

**Figure 3. Developmental assembly of the Golgi ribbon**. (A) Embryos of the sea urchin *Paracentrotus lividus* expressing fluorescent reporters of the Golgi apparatus and the plasma membrane (PM) were imaged at the indicated stages (hpf, hours post-fertilization; VEB, very early blastula; PHB, post-hatching blastula; BG, blastopore gastrula) by bright field and confocal microscopy (maximum intensity projections); right panels show magnifications of the middle panel insets; scale bars: 20 µm. (B) Maximum intensity projections of time-lapse confocal microscopy of an embryo microinjected as described in (A) and imaged at the indicated times (hpf); scale bar: 20 µm. (C) Number and size (median and interquartile range are shown) of Golgi objects in the embryo shown in (B) were measured; **, $p$ <0.01; ****, $p$ < 0.0001; Mann-Whitney test, compared to 8.5 hpf. (D) *Paracentrotus lividus*, (E) *Ciona robusta* and (F) *Branchiostoma lanceolatum* embryos were processed for electron microscopy at the indicated developmental stages; Golgi elements are outlined (isolated stacks in light ochre; linked stacks in light magenta); scale bars: 1 µm. See also Figure S4 and Movie S2.

## STAR METHODS

### Key Resources Table

| REAGENT or RESOURCE | SOURCE | IDENTIFIER |
|---|---|---|
| Antibodies | | |
| Mouse monoclonal anti-GM130 (clone 35) | BD Biosciences | Cat# 610823 |
| Bacterial strains | | |
| One Shot™ TOP10 Chemically Competent *E. coli* | ThermoFisher | Cat# C404010 |
| Chemicals | | |
| DMSO, Hybri-Max™ | Merck Millipore/Sigma-Aldrich | Cat# D2650 |
| Nocodazole | Merck Millipore/Sigma-Aldrich | Cat# M1404 |
| Commercial assays | | |

| | | |
|---|---|---|
| mMESSAGE mMACHINE T7 transcription kit | Invitrogen | Cat# AM1344 |
| NEBuilder HiFi DNA assembly cloning kit | NEB | Cat# E5520 |
| Q5® High-Fidelity DNA polymerase | NEB | Cat# M0491 |
| Experimental models: Cell lines | | |
| Human Umbilical Vein Endothelial Cells (HUVECs) pooled donors | Promocell | Cat. No. C-12203 |
| Experimental models: Organisms/strains | | |
| *Paracentrotus lividus – wild type* | Gulf of Naples, Italy | N/A |
| *Strongylocentrotus purpuratus – wild type* | California, USA | N/A |
| *Ciona robusta – wild type* | Gulf of Taranto, Italy | N/A |
| *Branchiostoma lanceolatum – wild type* | Argelès-sur-mer, France | N/A |
| *Platynereis dumerilii – wild type* | Cultured colony (founders from the Gulf of Naples) | N/A |
| *Calloria inconspicua – wild type* | Karitane Point, New Zealand | N/A |
| *Clytia hemisphaerica – wild type Z strain* | Cultured colony Leclère et al 2019 doi.org/10.1038/s41559-019-0833-2 | N/A |
| *Symsagittifera roscoffensis – wild type* | Roscoff, Brittany, France | N/A |
| *Parhyale hawaiensis – wild type* | Cultured colony (founders from the John G. Shedd Aquarium; Chicago; USA) | N/A |
| *Trichoplax adhaerens – wild type* | Cultured colony (founders from the Red Sea) | N/A |
| *Mnemiopsis leidyi – wild type* | Kristineberg, Sweden | N/A |
| *Oscarella carmela – wild type* | Carmel, California, USA | N/A |
| *Capsaspora owczarzaki – wild type strain* | Hertel, L.A., 2002 https://doi.org/10.1016/S0020-7519(02)00066-8 | ATCC30864 |
| Oligonucleotides | | |
| Assembly primers for plasmid pCineo_mEGFP_Giant-CT<br><br>Forward1: atacgactcactataggctagcATGGTGAGCAAGGGCGAG<br>Reverse1: acctgatccaccgccCTTGTACAGCTCGTCCATGC<br>Forward2: *ctgtacaag*ggcggtggatcaggtggaggatct*ACTC*CTATCATTGGCTC<br>Reverse2: gaggtaccacgcgtgaatTCATTACTATAGATGGCCC | This paper | N/A |

| | | |
|---|---|---|
| Assembly primers for plasmid pCineo_GalT_mCherry<br><br>Forward: ttaatacgactcactataggctagcATGAGGCTTCGGGAGCCG<br>Reverse: ctctagaggtaccacgcgtgaattcTTACTTGTACAGCTCGTCCATGC | This paper | N/A |
| Assembly primers for plasmid pCineo_mCherry_CAAX<br><br>Forward: ttaatacgactcactataggctagcATGGTGAGCAAGGGCGAG<br>Reverse: ctctagaggtaccacgcgtg*aattcttacataattacacactttgtctttgacttcttttcttcttttacc*CTTGTACAGCTCGTCCATGC | This paper | N/A |
| Recombinant DNA | | |
| Plasmid: pCineo vector | Promega | Cat# E1841 |
| Plasmid: pCineo_mEGFP_Giant-CT | This paper | N/A |
| Plasmid: pCineo_mCherry_CAAX | This paper | N/A |
| Plasmid: pCineo_GalT_mCherry | This paper | N/A |
| Software and algorithms | | |
| ImageJ | Schindelin, J. et al. 2012 https://doi.org/10.1038/nmeth.2019 | https://imagej.net/ij/index.html |
| Prism v9.4.1 | N/A | https://www.graphpad.com/ |
| BLAST | N/A | https://blast.ncbi.nlm.nih.gov/Blast.cgi |
| CLUSTAL-omega | Sievers, F. et al., 2011 https://doi.org/10.1038/msb.2011.75 | https://www.ebi.ac.uk/Tools/msa/clustalo/ |
| AliView | Larsson, A., 2014 https://doi.org/10.1093/bioinformatics/btu531 | https://ormbunkar.se/aliview/ |
| JalView | Waterhouse, A.M. et al., 2009 https://doi.org/10.1093/bioinformatics/btp033 | https://www.jalview.org/ |
| AlphaFold2 | Jumper, J. et al., 2021 DOI: 10.1038/s41586-021-03819-2. | https://www.deepmind.com/open-source/alphafold |
| ColabFold | Mirdita, M. et al., 2022 https://doi.org/10.1038/s41592-022-01488-1 | https://colab.research.google.com/github/sokrypton/ColabFold/blob/main/AlphaFold2.ipynb |
| Chimera | Pettersen E.F. et. al., 2004 https://doi.org/10.1002/jcc.20084 | http://www.cgl.ucsf.edu/chimera/ |

| | | |
|---|---|---|
| NEBuilder | N/A | https://nebuilder.neb.com/ |

## Resource availability

### Lead Contact

Further information and request for resources and reagents should be directed to and will be fulfilled by the lead contact, Francesco Ferraro (francesco.ferraro@szn.it)

### Materials availability

All reagents generated in this study are available from the lead contact upon request.

### Data and code availability

All data reported in this paper will be shared by the lead contact upon request.

This article does not report original code.

## Method details

### Experimental organisms

Animals were either sourced from the wild or lab cultured. Animal maintenance and treatments to obtain gametes for *in vitro* fertilization have been previously described[44,96-101]. *Parhyale hawaiensis* embryos were a gift by Michalis Averof (Institut de Génomique Fonctionnelle de Lyon, IGFL). *Symsagittifera roscoffensis* juveniles, cultured at 15°C, were processed within 3 days of hatching. The *Capsaspora owczarzaki* ATCC30864 strain, established in 2002[102]**,** was maintained in modified PYNFH medium (ATCC medium 1034) (https://www.atcc.org/products/327-x).

Details on the sourcing of the organisms used in this study are provided in the Key Resources Table.

### Cells

Human Umbilical Vein Endothelial Cells (HUVECs), expanded from pools of both sexes acquired from PromoCell, were maintained as described[103] and used within the 4$^{th}$ passage.

**Plasmids**

Primers were designed using the NEBuilder tool (http://nebuilder.neb.com/). PCR reactions for amplicon generation were carried out with Q5 High-Fidelity DNA Polymerase (NEB). For primer sequences refer to the Key Resources Table. pCineo_mEGFP_Giant-CT (labelled in the figures as mEGFP_Golgi). The plasmid encodes mEGFP in frame with a linker sequence (GGGSGGGS) and the 69 C-terminal amino acids of human Giantin for Golgi membrane targeting. The mEGFP coding sequence was amplified from pmEGFP-N1 vector (Clontech) with primers forward 1 (lower case: pCineo sequence; upper case mEGFP coding sequence) and reverse 1 (lower case: GGGS coding sequence; upper case: mEGFP coding sequence).

The sequence encoding the 69 C-terminal amino acids of human Giantin was amplified from human umbilical vein endothelial cell (HUVEC) cDNA with primers forward 2 (italics: mEGFP coding sequence; lower case: GGGSGGGS linker coding sequence; upper case: Giantin coding sequence) and reverse 2 (lower case: pCineo sequence; upper case: Giantin coding sequence and two stop codons).

pCineo_GalT_mCherry. A plasmid (the generous gift of Irina Kaverina, Vanderbilt School of Medicine) encoding the N-terminal 87 amino acids of galactosyl-transferase (GalT), which confer Golgi localization, in frame with mCherry was used as template to amplify the GalT_mCherry coding sequence using primers forward (lower case: pCineo sequence; upper case: GatT coding sequence) and reverse (lower case: pCineo sequence; upper case: GatT coding sequence).

pCineo_mCherry_CAAX (labelled in the figures as mCherry_PM). The sequence encoding mCherry in frame with the polybasic sequence and CAAX motif of human K-Ras (GKKKKKKSKTKCVIM) for targeting to the plasma membrane was generated by amplification of mCherry using the pmCherry-N1 (Clontech) plasmid as template and the following primers: forward (lower case: pCineo sequence; upper case: mCherry coding sequence) and reverse (lower case: pCineo sequence; italics: polybasic plus CAAX motif and stop codon coding sequence; upper case: mCherry coding sequence).

Amplicons and pCineo plasmid (linearized by NheI/EcoRI digestion) were assembled using the NEBuilder HiFi DNA assembly cloning kit (NEB) following the manufacturer instructions. Correct sequences were verified by Sanger sequencing.

### *In vitro* mRNA transcription and microinjections

Plasmids were linearized by digestion with NotI, a unique restriction site in the pCineo vector located downstream of the cloned sequences. One microgram of each linearized plasmid was used as template for *in vitro* transcription. Purified mRNAs were resuspended in DEPC-MilliQ water, their concentration measured**,** and their quality checked by agarose gel electrophoresis. mRNAs were aliquoted and stored at – 80°C until used.

Sea urchin eggs' jelly coat was dissolved by a short wash in acidic filtered sea water (1.5 mM citric acid in 0.22 µm filtered sea water, FSW). De-jellied eggs were then immobilized on 60 mm plastic dish lids pre-treated with 1% protamine sulphate (Merck, Sigma-Aldrich, P4380) in FSW. Eggs were then washed with FSW containing sodium para-amino benzoate (Sigma-Aldrich, A6928; 0.05% in FSW) to prevent hardening of the fertilization envelope. *In vitro* transcribed mRNAs were diluted to a final concentration of 300-500 ng/µL in 120 mM KCl/DEPC-water. Four to five pL of diluted mRNAs were injected per embryo, immediately after fertilization. Embryos were allowed to develop at 18°C.

### Confocal microscopy

*Paracentrotus lividus*. At the indicated times post-fertilization, embryo development was stopped by incubation with 0.2% paraformaldehyde in FSW, which kills the embryos while preserving mEGFP and mCherry fluorescence. Imaging was carried out within 16 h of formaldehyde treatment. Embryos laid on glass-bottom dishes containing FSW were imaged with an inverted 25x (NA 0.8) water immersion objective, using a Zeiss LSM700 system. Image stacks (z-step 1 µm) were acquired. Only one third to one half of the embryo volumes could be imaged at early stages, due to the opacity of yolk granules. At later stages (prism and pluteus) embryos were transparent and their whole volume was imaged.

For live imaging experiments, eggs were laid in FWS containing glass-bottom dishes pre-treated with protamine, fertilized, and then immediately microinjected with fluorescent reporter encoding mRNAs. Imaging was carried out as described above. Image stacks (z-step 1 µm) were acquired at 15 min intervals. Higher magnification imaging of embryos was carried out on mEGFP_Giant-CT (mEGFP_Golgi) microinjected embryos using a 40x (NA 1.10) water immersion objective with a Leica

SP8 confocal system. For presentation purposes, contrast-enhancement and gaussian-blur filtering were carried out (ImageJ) to the images shown. *HUVECs*. Cells were seeded on gelatin-coated 96-well plates (Nunclon surface©, NUNC) at 15.000 cells/well and grown in HGM medium for 24 h. After rinsing with fresh medium, cells were fed HGM containing 0.1% (vol:vol) DMSO (control treatment) or 33 µM (10 mg/mL) Nocodazole and incubated for hours before fixation with 4% formaldehyde in phosphate-buffered saline (PBS) for 10 minutes at RT. Fixed cells were permeabilized with 0.2% TX-100 (Merck, Sigma-Aldrich) in PBS for 10 min (RT) and then blocked with 5% BSA (Merck, Sigma-Aldrich) in PBS for 30 min (RT). The Golgi apparatus was immuno-labeled with an antibody raised against the Golgi marker GM130 (BD Biosciences), followed by incubation with Alexa Fluor 488 conjugated anti-mouse antibody (Life Technologies); primary and secondary antibodies were diluted in 1% BSA/0.02% TX-100/PBS. Nuclei were counterstained with Hoechst 33342 (Life Technologies), diluted in PBS, and images acquired using an Opera High Content Screening System (Perkin Elmer) through a 40x air objective (NA 0.6). Exclusively for presentation purposes, the confocal images of sea urchin embryos were subjected to gaussian blurring (ImageJ) of the Golgi and plasma membrane channels.

**Image analysis**

Golgi objects from confocal images were analyzed with ImageJ (https://imagej.nih.gov/ij/). The Golgi channel (8-bit) was selected, maximum intensity projection images generated and processed as follows.

Time course (Figure 3A). All images were subjected to background subtraction. Small Golgi objects observed at 2, 4 and 6 hpf were identified with the “find maxima” command and separated from each other by segmentation. The images of all time points were then subjected to thresholding and transformed into binary images. Golgi object number and size were then counted with the “analyze particles” command (area range was set at 0.25 – infinite $\mu m^2$). Three embryos per time point were analyzed. Time-lapse (Figure 3B). Image threshold was set automatically. At early time points, slight adjustments were done to correctly capture the size of most Golgi objects. For later time points, default threshold values were sufficient to correctly outline the size Golgi objects. After transformation into binary images, object number

and size were measured as described above. Numerical results were processed with Prism (Graphpad) for graph plotting and statistical analysis.

**Electron microscopy**

*Paracentrotus lividus*, *Branchiostoma lanceolatum* and *Ciona robusta* samples, maintained at 18°C, were collected at the indicated developmental stages and fixed at 4°C in 2% glutaraldehyde in filtered sea water (FSW). After fixation samples were first rinsed in FSW (6 x 10 min), then in Milli-Q water (3 x 10 min) and post-fixed with 1% osmium tetroxide and 1.5% potassium ferrocyanide (1 h, 4°C). Samples were then rinsed five times with Milli-Q water, dehydrated in a graded ethanol series, further substituted by propylene oxide and embedded in Epon 812 (TAAB, TAAB Laboratories Equipment Ltd, Berkshire, UK). Resin blocks were sectioned with a Ultracut UCT ultramicrotome (Leica, Vienna, Austria). Sections were placed on nickel grids and observed with a Zeiss LEO 912AB TEM (Zeiss, Oberkochen, Germany).

*Calloria inconspicua*. Three-lobed larvae were initially fixed in 2.5% glutardialdehyde buffered with 0.1 M sodium cacodylate solution (60 min at 5°C). A tiny amount ruthenium red solution was added to stain the extracellular matrix. Repeated rinsing in 0.1 M sodium cacodylate buffer was followed by post-fixation in 1% osmium tetroxide solution buffered with 0.1 M sodium cacodylate (40 min at 4°C). Dehydration with an acetone series and propylene oxide led to embedding in Araldite. Resin blocks were polymerized at 60°C for 48 hours. Ultrathin serial sections (70 nm) were cut on a Reichert Ultracut E microtome, placed on formvar-coated copper slot grids, and automatically stained with uranyl acetate and lead citrate in a LKB Ultrostainer. The sections were examined in Zeiss EM 10B and Zeiss EM 900 transmission electron microscopes.

*Parhyale hawaiensis.* Embryos were pre-fixed in 2.5% glutardialdehyde, 2% paraformaldehyde, 2% sucrose in sodium cacodylate buffer 0.1 M (SC buffer) overnight at 4°C. After several rinses in SC buffer at room temperature specimens were postfixed in 1% OsO4 in 0.1 M SC Buffer (2 hrs, room temperature), washed in SC buffer (1 hr) and dehydrated in an ethanol series. Ethanol-preserved specimens were sent to Berlin, transferred to 100% acetone and propylene oxide and subsequently embedded in araldite. Ultrathin sections were cut on a Leica EM UC7,

stained with Plano uranyl acetate replacement stain (UAR-EMS) and lead citrate and investigated in a LEO EM 906.

*Strongylocentrotus purpuratus, Platynereis dumerilii*, *Mnemiopsis leidyi*, *Oscarella carmela* and *Capsaspora owczarzaki* samples were high-pressure frozen, freeze substituted and processed as described[44,45,47,104-106].

*Trichoplax adhaerens.* Animals, alive of pre-fixed, were high-pressure frozen/freeze substituted and embedded in Epon. Sections (70 nm) were cut with using a Leica Ultracut UCT ultramicrotome.

*Symsagittifera roscoffensis*. Animals were processed within three days of hatching. The head of a hatchling was processed by high-pressure freezing. Freeze substitution was carried out in a solution of 1% osmium tetroxide and 0.1% uranyl acetate in acetone. A Leica Ultracut UCT was used to generate 60–80 nm sections, which were poststained in a 2% uranyl acetate/lead citrate solution and transferred to formvar-coated slit grids. Sections were imaged with a Tecnai 12 Biotwin TEM, using a fast-scan F214A CCD camera controlled by the SerialEM software (Boulder Lab). Digital image stacks were imported into the TrakEM2 package.

*Clytia hemisphaerica*. Individual ovaries were high-pressure frozen with a Wohlwend Compact 03 high-pressure freezing machine (http://www.wohlwend-hpf.ch) using sea water as the freezing medium and then transferred to a frozen solution of 2% osmium in acetone under liquid nitrogen. The ovaries were freeze-substituted in a Leica AFS2 freeze-substitution machine (https://www.leica-microsystems.com) using the following program: -90°C for 18 hours, -90°C to -30°C with a slope of 5°C/hour, -30°C for 12 hours, -30°C to 0°C with a slope of 5°C/hour. Samples were removed from the AFS chamber and allowed to reach room temperature. This was followed by 5 acetone washes for 5 minutes each. Ovaries were infiltrated with Polybed resin in a series of steps as follows: 1:3 resin to acetone overnight, 1:1 resin to acetone for 6 hours, 3:1 resin to acetone overnight, 100% resin for 6 hours followed by embedment in molds in fresh 100% resin and curation at 60°C for 2 days. Polymerized samples were then trimmed using an ultramicrotome to get the entire cross-section of the ovary. Serial 60 nm sections were collected using an Automated Tape-Collecting Ultramicrotome, mapped, and imaged with a Zeiss Sigma FE-SEM as described previously[107].

**Homology search**

Canonical human GRASP (GRASP65 and GRASP55) and Golgin-45 amino acid sequences (Data S1 and S2) were used as initial queries. Homologs were searched in the target species using Basic Local Alignment Search Tool, BLAST, (BLASTp and TBLASTn) in available databases (Uniprot, NCBI, Ensembl). For specific target species, the search was carried out in dedicated databases (*Amphiura filiformis*: http://www.echinonet.org.uk/blast/; *Mnemiopsis leidyi*: https://research.nhgri.nih.gov/mnemiopsis/sequenceserver/; *Nematostella vectensis*: http://marimba.obs-vlfr.fr/blast; unicellular holozoans: https://protists.ensembl.org). Target genomes and, whenerver available, transcritpomes were interrogated. Hits with the lowest E-value and highest query coverage were selected as candidate homologs and validated when by reverse BLAST on the human proteome the query was retrieved as the highest scoring. If this approach did not return a hit, homologs of evolutionarily closer species were used as queries. Further validation of homology was obtained by subjecting the hits to sequence and structural analysis with InterProScan (https://www.ebi.ac.uk/interpro/search/sequence/) and by multiple sequence alignment with AliView and JalView to verify regions of sequence similarity.

**Structure modelling**

Models of complexes between conspecific GRASP/Golgin-45 pairs were built with the Colab implementation of AlphaFold2[76], using MMseqs2 to generate multiple sequences alignments[108]. To obtain reliable predictions of the protein-peptide complexes, AlphaFold-Multimer version v2 was used, with 12 recycles for the generation of each model[109]. Complexes were built without the use of structural templates and without Amber refinement as this step does not introduce substantial improvement, while significantly increasing computational time.

**Note about the phylogenetic trees**. Whether sponges or ctenophores or placozoans are the sister group to all other animals remains an unsettled issue[110-120]; for this reason we drew the holozoan tree of life as a polytomy of these three taxa in Figures 1K, 2E and in the graphical abstract. The animal silhouettes used in the graphical abstract were obtained from the public domain (http://phylopic.org), when not covered by copyright, or drawn by F.F.

## References


1. Glick, B.S., and Nakano, A. (2009). Membrane traffic within the Golgi apparatus. Annual review of cell and developmental biology *25*, 113-132.

2. Jackson, C.L. (2009). Mechanisms of transport through the Golgi complex. Journal of cell science *122*, 443-452. 10.1242/jcs.032581.

3. Di Martino, R., Sticco, L., and Luini, A. (2019). Regulation of cargo export and sorting at the trans-Golgi network. FEBS Lett *593*, 2306-2318. 10.1002/1873-3468.13572.

4. Taniguchi, M., and Yoshida, H. (2017). TFE3, HSP47, and CREB3 Pathways of the Mammalian Golgi Stress Response. Cell structure and function *42*, 27-36. 10.1247/csf.16023.

5. Machamer, C.E. (2015). The Golgi complex in stress and death. Frontiers in neuroscience *9*, 421. 10.3389/fnins.2015.00421.

6. Chiu, R., Novikov, L., Mukherjee, S., and Shields, D. (2002). A caspase cleavage fragment of p115 induces fragmentation of the Golgi apparatus and apoptosis. The Journal of cell biology *159*, 637-648. 10.1083/jcb.200208013.

7. Mukherjee, S., Chiu, R., Leung, S.M., and Shields, D. (2007). Fragmentation of the Golgi apparatus: an early apoptotic event independent of the cytoskeleton. Traffic (Copenhagen, Denmark) *8*, 369-378. 10.1111/j.1600-0854.2007.00542.x.

8. Tao, Y., Yang, Y., Zhou, R., and Gong, T. (2020). Golgi Apparatus: An Emerging Platform for Innate Immunity. Trends Cell Biol *30*, 467-477. 10.1016/j.tcb.2020.02.008.

9. Eisenberg-Lerner, A., Benyair, R., Hizkiahou, N., Nudel, N., Maor, R., Kramer, M.P., Shmueli, M.D., Zigdon, I., Cherniavsky Lev, M., Ulman, A., et al. (2020). Golgi organization is regulated by proteasomal degradation. Nature communications *11*, 409. 10.1038/s41467-019-14038-9.

10. Farber-Katz, S.E., Dippold, H.C., Buschman, M.D., Peterman, M.C., Xing, M., Noakes, C.J., Tat, J., Ng, M.M., Rahajeng, J., Cowan, D.M., et al. (2014). DNA damage triggers Golgi dispersal via DNA-PK and GOLPH3. Cell *156*, 413-427. 10.1016/j.cell.2013.12.023.

11. Catara, G., Grimaldi, G., Schembri, L., Spano, D., Turacchio, G., Lo Monte, M., Beccari, A.R., Valente, C., and Corda, D. (2017). PARP1-produced poly-ADP-ribose causes the PARP12 translocation to stress granules and impairment of Golgi complex functions. Sci Rep *7*, 14035. 10.1038/s41598-017-14156-8.

12. Mazzarello, P., Garbarino, C., and Calligaro, A. (2009). How Camillo Golgi became "the Golgi". FEBS Lett *583*, 3732-3737. 10.1016/j.febslet.2009.10.018.

13. Wei, J.H., and Seemann, J. (2010). Unraveling the Golgi ribbon. Traffic (Copenhagen, Denmark) *11*, 1391-1400.

14. Wei, J.H., and Seemann, J. (2017). Golgi ribbon disassembly during mitosis, differentiation and disease progression. Curr Opin Cell Biol *47*, 43-51. 10.1016/j.ceb.2017.03.008.

15. Gosavi, P., and Gleeson, P.A. (2017). The Function of the Golgi Ribbon Structure - An Enduring Mystery Unfolds! Bioessays *39*. 10.1002/bies.201700063.

16. Ayala, I., Mascanzoni, F., and Colanzi, A. (2020). The Golgi ribbon: mechanisms of maintenance and disassembly during the cell cycle. Biochem Soc Trans *48*, 245-256. 10.1042/BST20190646.

17. Bellouze, S., Baillat, G., Buttigieg, D., de la Grange, P., Rabouille, C., and Haase, G. (2016). Stathmin 1/2-triggered microtubule loss mediates Golgi fragmentation in mutant SOD1 motor neurons. Molecular neurodegeneration *11*, 43. 10.1186/s13024-016-0111-6.

18. Rabouille, C., and Haase, G. (2015). Editorial: Golgi Pathology in Neurodegenerative Diseases. Frontiers in neuroscience *9*, 489. 10.3389/fnins.2015.00489.

19. Joshi, G., Chi, Y., Huang, Z., and Wang, Y. (2014). Abeta-induced Golgi fragmentation in Alzheimer's disease enhances Abeta production. Proceedings of the National Academy of Sciences of the United States of America *111*, E1230-1239. 10.1073/pnas.1320192111.

20. Bui, S., Mejia, I., Diaz, B., and Wang, Y. (2021). Adaptation of the Golgi Apparatus in Cancer Cell Invasion and Metastasis. Frontiers in cell and developmental biology *9*, 806482. 10.3389/fcell.2021.806482.

21. Cortese, M., Lee, J.Y., Cerikan, B., Neufeldt, C.J., Oorschot, V.M.J., Kohrer, S., Hennies, J., Schieber, N.L., Ronchi, P., Mizzon, G., et al. (2020). Integrative Imaging Reveals SARS-CoV-2-Induced Reshaping of Subcellular Morphologies. Cell Host Microbe. 10.1016/j.chom.2020.11.003.

22. Hansen, M.D., Johnsen, I.B., Stiberg, K.A., Sherstova, T., Wakita, T., Richard, G.M., Kandasamy, R.K., Meurs, E.F., and Anthonsen, M.W. (2017). Hepatitis C virus triggers Golgi fragmentation and autophagy through the immunity-related GTPase M. Proceedings of the National Academy of Sciences of the United States of America *114*, E3462-E3471. 10.1073/pnas.1616683114.

23. Haukedal, H., Corsi, G.I., Gadekar, V.P., Doncheva, N.T., Kedia, S., de Haan, N., Chandrasekaran, A., Jensen, P., Schionning, P., Vallin, S., et al. (2023). Golgi fragmentation - One of the earliest organelle phenotypes in Alzheimer's disease neurons. Frontiers in neuroscience *17*, 1120086. 10.3389/fnins.2023.1120086.

24. Eldon, E.D., Montpetit, I.C., Nguyen, T., Decker, G., Valdizan, M.C., Klein, W.H., and Brandhorst, B.P. (1990). Localization of the sea urchin Spec3 protein to cilia and Golgi complexes of embryonic ectoderm cells. Genes Dev *4*, 111-122. 10.1101/gad.4.1.111.

25. Terasaki, M. (2000). Dynamics of the endoplasmic reticulum and golgi apparatus during early sea urchin development. Molecular biology of the cell *11*, 897-914.

26. Cole, N.B.S., C.L.; Sciaky, N.; Terasaki, M.; Edidin, M.; Lippincott-Schwartz, J. (1996). Diffusional mobility of Golgi proteins in membranes of living cells. Science (New York, N.Y *273*, 797-801. 10.1126/science.273.5276.797

27. Ladinsky, M.S., Mastronarde, D.N., McIntosh, J.R., Howell, K.E., and Staehelin, L.A. (1999). Golgi structure in three dimensions: functional insights from the normal rat kidney cell. The Journal of cell biology *144*, 1135-1149.

28. Kondylis, V., van Nispen tot Pannerden, H.E., Herpers, B., Friggi-Grelin, F., and Rabouille, C. (2007). The golgi comprises a paired stack that is separated at G2 by modulation of the actin cytoskeleton through Abi and Scar/WAVE. Developmental cell *12*, 901-915.

29. Yano, H., Yamamoto-Hino, M., Abe, M., Kuwahara, R., Haraguchi, S., Kusaka, I., Awano, W., Kinoshita-Toyoda, A., Toyoda, H., and Goto, S. (2005). Distinct functional units of the Golgi complex in Drosophila cells. Proceedings of the National Academy of Sciences of the United States of America *102*, 13467-13472. 10.1073/pnas.0506681102.

30. Page, K.M., McCormack, J.J., Lopes-da-Silva, M., Patella, F., Harrison-Lavoie, K., Burden, J.J., Quah, Y.B., Scaglioni, D., Ferraro, F., and Cutler, D.F. (2022). Structure modeling hints at a granular organization of the Golgi ribbon. BMC biology *20*, 111. 10.1186/s12915-022-01305-3.

31. Lu, Z., Joseph, D., Bugnard, E., Zaal, K.J., and Ralston, E. (2001). Golgi complex reorganization during muscle differentiation: visualization in living cells and mechanism. Molecular biology of the cell *12*, 795-808.

32. Gunn, P.A., Gliddon, B.L., Londrigan, S.L., Lew, A.M., van Driel, I.R., and Gleeson, P.A. (2011). The Golgi apparatus in the endomembrane-rich gastric parietal cells exist as functional stable mini-stacks dispersed throughout the cytoplasm. Biology of the cell *103*, 559-572. 10.1042/BC20110074.

33. Koga, D., and Ushiki, T. (2006). Three-dimensional ultrastructure of the Golgi apparatus in different cells: high-resolution scanning electron microscopy of osmium-macerated tissues. Arch Histol Cytol *69*, 357-374. 10.1679/aohc.69.357.

34. Ramón y Cajal, S. (1903). Sobre la existencia de un aparato tubuliforme en el protoplasma de las células nerviosas y epiteliales de la lombriz de tierra. Boletín de la Sociedad Española de Historia Natural, 395-398.

35. Perroncito, A. (1910). Contributo allo studio della biologia cellulare – mitocondri, cromidii e apparato reticolare interno nelle cellule spermatiche. Memorie della R. Accademia dei Lincei; Classe di Scienze Fisiche, Matematiche e Naturali *VIII*, 226-261.

36. Mollenhauer, H.H., and Morre, D.J. (1998). The tubular network of the Golgi apparatus. Histochem Cell Biol *109*, 533-543. 10.1007/s004180050253.

37. Meek, G.A., and Bradbury, S. (1963). Localization of thiamine pyrophosphatase activity in the golgi apparatus of a mollusc, Helix aspersa. The Journal of cell biology *18*, 73-85. 10.1083/jcb.18.1.73.

38. Sato, M., Saegusa, K., Sato, K., Hara, T., Harada, A., and Sato, K. (2011). Caenorhabditis elegans SNAP-29 is required for organellar integrity of the endomembrane system and general exocytosis in intestinal epithelial cells. Molecular biology of the cell *22*, 2579-2587. 10.1091/mbc.E11-04-0279.

39. Witte, K., Schuh, A.L., Hegermann, J., Sarkeshik, A., Mayers, J.R., Schwarze, K., Yates, J.R., 3rd, Eimer, S., and Audhya, A. (2011). TFG-1 function in protein secretion and oncogenesis. Nat Cell Biol *13*, 550-558. 10.1038/ncb2225.

40. Kuterbach, D.A., and Walcott, B. (1986). Iron-containing cells in the honey-bee (Apis mellifera). I. Adult morphology and physiology. J Exp Biol *126*, 375-387. 10.1242/jeb.126.1.375.

41. Griffiths, G.W., and Beck, S.D. (1975). Ultrastructure of pea aphid mycetocytes: evidence for symbiote secretion. Cell Tissue Res *159*, 351-367. 10.1007/BF00221782.

42. Rolls, M.M., Marquardt, M.T., Kielian, M., and Machamer, C.E. (1997). Cholesterol-independent targeting of Golgi membrane proteins in insect cells. Molecular biology of the cell *8*, 2111-2118. 10.1091/mbc.8.11.2111.

43. Van-Praët, M. (1985). Nutrition of Sea Anemones. Advances in Marine Biology *22*, 65-99. https://doi.org/10.1016/S0065-2881(08)60050-4.

44. Sachkova, M.Y., Nordmann, E.L., Soto-Angel, J.J., Meeda, Y., Gorski, B., Naumann, B., Dondorp, D., Chatzigeorgiou, M., Kittelmann, M., and Burkhardt, P. (2021). Neuropeptide repertoire and 3D anatomy of the ctenophore nervous system. Curr Biol *31*, 5274-5285 e5276. 10.1016/j.cub.2021.09.005.

45. Burkhardt, P., Medhus, A., Digel, L., Naumann, B., Soto-Àngel, J.J., Nordmann, E.-L., Sachkova, M.Y., and Kittelmann, M. (2022). Syncytial nerve net in a ctenophore sheds new light on the early evolution of nervous systems. bioRxiv, 2022.2008.2014.503905. 10.1101/2022.08.14.503905.

46. Romanova, D.Y., Varoqueaux, F., Daraspe, J., Nikitin, M.A., Eitel, M., Fasshauer, D., and Moroz, L.L. (2021). Hidden cell diversity in Placozoa: ultrastructural insights from Hoilungia hongkongensis. Cell Tissue Res *385*, 623-637. 10.1007/s00441-021-03459-y.

47. Laundon, D., Larson, B.T., McDonald, K., King, N., and Burkhardt, P. (2019). The architecture of cell differentiation in choanoflagellates and sponge choanocytes. PLoS biology *17*, e3000226. 10.1371/journal.pbio.3000226.

48. Burkhardt, P., Stegmann, C.M., Cooper, B., Kloepper, T.H., Imig, C., Varoqueaux, F., Wahl, M.C., and Fasshauer, D. (2011). Primordial neurosecretory apparatus identified in the choanoflagellate Monosiga brevicollis. Proceedings of the National Academy of Sciences of the United States of America *108*, 15264-15269. 10.1073/pnas.1106189108.

49. Harrisson, F.W., and De Vos, L. (1991). Porifera (Willey-Liss).

50. Kulkarni-Gosavi, P., Makhoul, C., and Gleeson, P.A. (2019). Form and function of the Golgi apparatus: scaffolds, cytoskeleton and signalling. FEBS Lett *593*, 2289-2305. 10.1002/1873-3468.13567.

51. Munro, S. (2011). The golgin coiled-coil proteins of the Golgi apparatus. Cold Spring Harb Perspect Biol *3*. 10.1101/cshperspect.a005256.

52. Witkos, T.M., and Lowe, M. (2015). The Golgin Family of Coiled-Coil Tethering Proteins. Frontiers in cell and developmental biology *3*, 86. 10.3389/fcell.2015.00086.

53. Lowe, M. (2019). The Physiological Functions of the Golgin Vesicle Tethering Proteins. Frontiers in cell and developmental biology *7*, 94. 10.3389/fcell.2019.00094.

54. Bekier, M.E., 2nd, Wang, L., Li, J., Huang, H., Tang, D., Zhang, X., and Wang, Y. (2017). Knockout of the Golgi stacking proteins GRASP55 and GRASP65 impairs Golgi structure and function. Molecular biology of the cell *28*, 2833-2842. 10.1091/mbc.E17-02-0112.

55. Grond, R., Veenendaal, T., Duran, J.M., Raote, I., van Es, J.H., Corstjens, S., Delfgou, L., El Haddouti, B., Malhotra, V., and Rabouille, C. (2020). The function of GORASPs in Golgi apparatus organization in vivo. The Journal of cell biology *219*. 10.1083/jcb.202004191.

56. Zhang, Y., and Seemann, J. (2021). Rapid degradation of GRASP55 and GRASP65 reveals their immediate impact on the Golgi structure. The Journal of cell biology *220*. 10.1083/jcb.202007052.

57. Kinseth, M.A., Anjard, C., Fuller, D., Guizzunti, G., Loomis, W.F., and Malhotra, V. (2007). The Golgi-associated protein GRASP is required for unconventional protein secretion during development. Cell *130*, 524-534. 10.1016/j.cell.2007.06.029.

58. Zhang, X., Wang, L., Lak, B., Li, J., Jokitalo, E., and Wang, Y. (2018). GRASP55 Senses Glucose Deprivation through O-GlcNAcylation to Promote Autophagosome-Lysosome Fusion. Developmental cell *45*, 245-261 e246. 10.1016/j.devcel.2018.03.023.

59. Nuchel, J., Tauber, M., Nolte, J.L., Morgelin, M., Turk, C., Eckes, B., Demetriades, C., and Plomann, M. (2021). An mTORC1-GRASP55 signaling axis controls unconventional secretion to reshape the extracellular proteome upon stress. Mol Cell *81*, 3275-3293 e3212. 10.1016/j.molcel.2021.06.017.

60. Rabouille, C., and Linstedt, A.D. (2016). GRASP: A Multitasking Tether. Frontiers in cell and developmental biology *4*, 1. 10.3389/fcell.2016.00001.

61. Barr, F.A., Puype, M., Vandekerckhove, J., and Warren, G. (1997). GRASP65, a protein involved in the stacking of Golgi cisternae. Cell *91*, 253-262.

62. Shorter, J., Watson, R., Giannakou, M.E., Clarke, M., Warren, G., and Barr, F.A. (1999). GRASP55, a second mammalian GRASP protein involved in the stacking of Golgi cisternae in a cell-free system. The EMBO journal *18*, 4949-4960. 10.1093/emboj/18.18.4949.

63. Xiang, Y., and Wang, Y. (2010). GRASP55 and GRASP65 play complementary and essential roles in Golgi cisternal stacking. The Journal of cell biology *188*, 237-251. 10.1083/jcb.200907132.

64. Kuo, A., Zhong, C., Lane, W.S., and Derynck, R. (2000). Transmembrane transforming growth factor-alpha tethers to the PDZ domain-containing, Golgi membrane-associated protein p59/GRASP55. The EMBO journal *19*, 6427-6439. 10.1093/emboj/19.23.6427.

65. Barr, F.A., Nakamura, N., and Warren, G. (1998). Mapping the interaction between GRASP65 and GM130, components of a protein complex involved in the stacking of Golgi cisternae. The EMBO journal *17*, 3258-3268. 10.1093/emboj/17.12.3258.

66. Short, B., Preisinger, C., Korner, R., Kopajtich, R., Byron, O., and Barr, F.A. (2001). A GRASP55-rab2 effector complex linking Golgi structure to membrane traffic. The Journal of cell biology *155*, 877-883. 10.1083/jcb.200108079.

67. Sengupta, D., Truschel, S., Bachert, C., and Linstedt, A.D. (2009). Organelle tethering by a homotypic PDZ interaction underlies formation of the Golgi membrane network. The Journal of cell biology *186*, 41-55. 10.1083/jcb.200902110.

68. Bachert, C., and Linstedt, A.D. (2010). Dual anchoring of the GRASP membrane tether promotes trans pairing. The Journal of biological chemistry *285*, 16294-16301. 10.1074/jbc.M110.116129.

69. Heinrich, F., Nanda, H., Goh, H.Z., Bachert, C., Losche, M., and Linstedt, A.D. (2014). Myristoylation restricts orientation of the GRASP domain on membranes and promotes membrane tethering. The Journal of biological chemistry *289*, 9683-9691. 10.1074/jbc.M113.543561.

70. Malsam, J., Satoh, A., Pelletier, L., and Warren, G. (2005). Golgin tethers define subpopulations of COPI vesicles. Science (New York, N.Y *307*, 1095-1098. 10.1126/science.1108061.

71. Wong, M., and Munro, S. (2014). Membrane trafficking. The specificity of vesicle traffic to the Golgi is encoded in the golgin coiled-coil proteins. Science (New York, N.Y *346*, 1256898. 10.1126/science.1256898.

72. Wong, M., Gillingham, A.K., and Munro, S. (2017). The golgin coiled-coil proteins capture different types of transport carriers via distinct N-terminal motifs. BMC biology *15*, 3. 10.1186/s12915-016-0345-3.

73. Barlow, L.D., Nyvltova, E., Aguilar, M., Tachezy, J., and Dacks, J.B. (2018). A sophisticated, differentiated Golgi in the ancestor of eukaryotes. BMC biology *16*, 27. 10.1186/s12915-018-0492-9.

74. Zhao, J., Li, B., Huang, X., Morelli, X., and Shi, N. (2017). Structural Basis for the Interaction between Golgi Reassembly-stacking Protein GRASP55 and Golgin45. The Journal of biological chemistry *292*, 2956-2965. 10.1074/jbc.M116.765990.

75. Jumper, J., Evans, R., Pritzel, A., Green, T., Figurnov, M., Ronneberger, O., Tunyasuvunakool, K., Bates, R., Zidek, A., Potapenko, A., et al. (2021). Highly

accurate protein structure prediction with AlphaFold. Nature *596*, 583-589. 10.1038/s41586-021-03819-2.

76. Mirdita, M., Schutze, K., Moriwaki, Y., Heo, L., Ovchinnikov, S., and Steinegger, M. (2022). ColabFold: making protein folding accessible to all. Nat Methods *19*, 679-682. 10.1038/s41592-022-01488-1.

77. Guo, H.B., Perminov, A., Bekele, S., Kedziora, G., Farajollahi, S., Varaljay, V., Hinkle, K., Molinero, V., Meister, K., Hung, C., et al. (2022). AlphaFold2 models indicate that protein sequence determines both structure and dynamics. Sci Rep *12*, 10696. 10.1038/s41598-022-14382-9.

78. Tsaban, T., Varga, J.K., Avraham, O., Ben-Aharon, Z., Khramushin, A., and Schueler-Furman, O. (2022). Harnessing protein folding neural networks for peptide-protein docking. Nature communications *13*, 176. 10.1038/s41467-021-27838-9.

79. Ayala, I., and Colanzi, A. (2022). Structural Organization and Function of the Golgi Ribbon During Cell Division. Frontiers in cell and developmental biology *10*, 925228. 10.3389/fcell.2022.925228.

80. Thyberg, J., and Moskalewski, S. (1985). Microtubules and the organization of the Golgi complex. Exp Cell Res *159*, 1-16.

81. Cole, N.B., Sciaky, N., Marotta, A., Song, J., and Lippincott-Schwartz, J. (1996). Golgi dispersal during microtubule disruption: regeneration of Golgi stacks at peripheral endoplasmic reticulum exit sites. Molecular biology of the cell *7*, 631-650.

82. Kiyonari, H., Kaneko, M., Abe, T., Shioi, G., Aizawa, S., Furuta, Y., and Fujimori, T. (2019). Dynamic organelle localization and cytoskeletal reorganization during preimplantation mouse embryo development revealed by live imaging of genetically encoded fluorescent fusion proteins. Genesis *57*, e23277. 10.1002/dvg.23277.

83. Tamarin, A., and Keller, P.J. (1972). An ultrastructural study of the byssal thread forming system in Mytilus. J Ultrastruct Res *40*, 401-416. 10.1016/s0022-5320(72)90110-4.

84. Mendes, L.F.S., Batista, M.R.B., Kava, E., Bleicher, L., Micheletto, M.C., and Costa-Filho, A.J. (2022). Resurrecting Golgi proteins to grasp Golgi ribbon formation and self-association under stress. Int J Biol Macromol *194*, 264-275. 10.1016/j.ijbiomac.2021.11.173.

85. Rambourg, A., and Clermont, Y. (1997). Three-dimensional structure of the Golgi apparatus in mammalian cells. In The Golgi Apparatus, E.G. Berger, and J. Roth, eds. (Birkhäuser, Basel), pp. 37-61. 10.1007/978-3-0348-8876-9_2.

86. Mendes, L.F.S., Fontana, N.A., Reddy, S.T., Uversky, V.N., and Costa-Filho, A.J. (2020). The exquisite structural biophysics of the Golgi Reassembly and Stacking Proteins. Int J Biol Macromol *164*, 3632-3644. 10.1016/j.ijbiomac.2020.08.203.

87. Houliston, E., Leclere, L., Munro, C., Copley, R.R., and Momose, T. (2022). Past, present and future of Clytia hemisphaerica as a laboratory jellyfish. Curr Top Dev Biol *147*, 121-151. 10.1016/bs.ctdb.2021.12.014.

88. Darling, J.A., Reitzel, A.R., Burton, P.M., Mazza, M.E., Ryan, J.F., Sullivan, J.C., and Finnerty, J.R. (2005). Rising starlet: the starlet sea anemone, Nematostella vectensis. Bioessays *27*, 211-221. 10.1002/bies.20181.

89. Ozpolat, B.D., Randel, N., Williams, E.A., Bezares-Calderon, L.A., Andreatta, G., Balavoine, G., Bertucci, P.Y., Ferrier, D.E.K., Gambi, M.C., Gazave, E., et al. (2021). The Nereid on the rise: Platynereis as a model system. Evodevo *12*, 10. 10.1186/s13227-021-00180-3.

90. Knoll, A.H. (2011). The Multiple Origins of Complex Multicellularity. Annual Review of Earth and Planetary Sciences *39*, 217–239. 10.1146/annurev.earth.031208.100209.

91. Vildanova, M.S., Wang, W., and Smirnova, E.A. (2014). Specific organization of Golgi apparatus in plant cells. Biochemistry (Mosc) *79*, 894-906. 10.1134/S0006297914090065.

92. Staehelin, L.A., and Kang, B.H. (2008). Nanoscale architecture of endoplasmic reticulum export sites and of Golgi membranes as determined by electron tomography. Plant Physiol *147*, 1454-1468. 10.1104/pp.108.120618.

93. Bracker, C.E.M., D.J.; Grove, S.N.; (1996). Structure, differentiation, and multiplication of Golgi apparatus in fungal hyphae. Protoplasma *194*, 250-274.

94. Gillingham, A.K., and Munro, S. (2016). Finding the Golgi: Golgin Coiled-Coil Proteins Show the Way. Trends Cell Biol *26*, 399-408. 10.1016/j.tcb.2016.02.005.

95. Tie, H.C., Ludwig, A., Sandin, S., and Lu, L. (2018). The spatial separation of processing and transport functions to the interior and periphery of the Golgi stack. Elife *7*. 10.7554/eLife.41301.

96. Paganos, P., Caccavale, F., La Vecchia, C., D'Aniello, E., D'Aniello, S., and Arnone, M.I. (2022). FISH for All: A Fast and Efficient Fluorescent In situ Hybridization (FISH) Protocol for Marine Embryos and Larvae. Front Physiol *13*, 878062. 10.3389/fphys.2022.878062.

97. Reed, C.G. (1987). Reproduction and development of marine invertebrates of the northern Pacific coast. Phylum Brachiopoda. (University of Washington Press).

98. Nislow, C. (1994). Reproduction and development of marine invertebrates. Cellular dynamics during the early development of an articulate brachiopod. (Johns Hopkins University Press, ).

99. Schierwater, B. (2005). My favorite animal, Trichoplax adhaerens. Bioessays *27*, 1294-1302. 10.1002/bies.20320.

100. Browne, W.E., Price, A.L., Gerberding, M., and Patel, N.H. (2005). Stages of embryonic development in the amphipod crustacean, Parhyale hawaiensis. Genesis *42*, 124-149. 10.1002/gene.20145.

101. Leclere, L., Horin, C., Chevalier, S., Lapebie, P., Dru, P., Peron, S., Jager, M., Condamine, T., Pottin, K., Romano, S., et al. (2019). The genome of the jellyfish

Clytia hemisphaerica and the evolution of the cnidarian life-cycle. Nat Ecol Evol *3*, 801-810. 10.1038/s41559-019-0833-2.

102. Hertel, L.A., Bayne, C.J., and Loker, E.S. (2002). The symbiont Capsaspora owczarzaki, nov. gen. nov. sp., isolated from three strains of the pulmonate snail Biomphalaria glabrata is related to members of the Mesomycetozoea. Int J Parasitol *32*, 1183-1191. 10.1016/s0020-7519(02)00066-8.

103. Ferraro, F., Patella, F., Costa, J.R., Ketteler, R., Kriston-Vizi, J., and Cutler, D.F. (2020). Modulation of endothelial organelle size as an antithrombotic strategy. J Thromb Haemost. 10.1111/jth.15084.

104. Paganos, P., Ronchi, P., Carl, J., Mizzon, G., Martinez, P., Benvenuto, G., and Arnone, M.I. (2022). Integrating single cell transcriptomics and volume electron microscopy confirms the presence of pancreatic acinar-like cells in sea urchins. Frontiers in cell and developmental biology *10*, 991664. 10.3389/fcell.2022.991664.

105. Sebe-Pedros, A., Irimia, M., Del Campo, J., Parra-Acero, H., Russ, C., Nusbaum, C., Blencowe, B.J., and Ruiz-Trillo, I. (2013). Regulated aggregative multicellularity in a close unicellular relative of metazoa. Elife *2*, e01287. 10.7554/eLife.01287.

106. Verasztó, C., Jasek, S., Gühmann, M., Shahidi, R., Ueda, N., Beard, J.D., Mendes, S., Heinz, K., Bezares-Calderón, L.A., Williams, E., and Jékely, G. (2020). Whole-animal connectome and cell-type complement of the three-segmented Platynereis dumerilii larva. biorXiv. https://doi.org/10.1101/2020.08.21.260984

107. Baena, V., Schalek, R.L., Lichtman, J.W., and Terasaki, M. (2019). Serial-section electron microscopy using automated tape-collecting ultramicrotome (ATUM). Methods in cell biology *152*, 41-67. 10.1016/bs.mcb.2019.04.004.

108. Steinegger, M., and Soding, J. (2017). MMseqs2 enables sensitive protein sequence searching for the analysis of massive data sets. Nature biotechnology *35*, 1026-1028. 10.1038/nbt.3988.

109. Johansson-Akhe, I., and Wallner, B. (2022). Improving peptide-protein docking with AlphaFold-Multimer using forced sampling. Front Bioinform *2*, 959160. 10.3389/fbinf.2022.959160.

110. Philippe, H., Derelle, R., Lopez, P., Pick, K., Borchiellini, C., Boury-Esnault, N., Vacelet, J., Renard, E., Houliston, E., Queinnec, E., et al. (2009). Phylogenomics revives traditional views on deep animal relationships. Curr Biol *19*, 706-712. 10.1016/j.cub.2009.02.052.

111. Pisani, D., Pett, W., Dohrmann, M., Feuda, R., Rota-Stabelli, O., Philippe, H., Lartillot, N., and Worheide, G. (2015). Genomic data do not support comb jellies as the sister group to all other animals. Proceedings of the National Academy of Sciences of the United States of America *112*, 15402-15407. 10.1073/pnas.1518127112.

112. Feuda, R., Dohrmann, M., Pett, W., Philippe, H., Rota-Stabelli, O., Lartillot, N., Worheide, G., and Pisani, D. (2017). Improved Modeling of Compositional

Heterogeneity Supports Sponges as Sister to All Other Animals. Curr Biol *27*, 3864-3870 e3864. 10.1016/j.cub.2017.11.008.

113. Simion, P., Philippe, H., Baurain, D., Jager, M., Richter, D.J., Di Franco, A., Roure, B., Satoh, N., Queinnec, E., Ereskovsky, A., et al. (2017). A Large and Consistent Phylogenomic Dataset Supports Sponges as the Sister Group to All Other Animals. Curr Biol *27*, 958-967. 10.1016/j.cub.2017.02.031.

114. Redmond, A.K., and McLysaght, A. (2021). Evidence for sponges as sister to all other animals from partitioned phylogenomics with mixture models and recoding. Nature communications *12*, 1783. 10.1038/s41467-021-22074-7.

115. Ryan, J.F., Pang, K., Schnitzler, C.E., Nguyen, A.D., Moreland, R.T., Simmons, D.K., Koch, B.J., Francis, W.R., Havlak, P., Program, N.C.S., et al. (2013). The genome of the ctenophore Mnemiopsis leidyi and its implications for cell type evolution. Science (New York, N.Y *342*, 1242592. 10.1126/science.1242592.

116. Moroz, L.L., Kocot, K.M., Citarella, M.R., Dosung, S., Norekian, T.P., Povolotskaya, I.S., Grigorenko, A.P., Dailey, C., Berezikov, E., Buckley, K.M., et al. (2014). The ctenophore genome and the evolutionary origins of neural systems. Nature *510*, 109-114. 10.1038/nature13400.

117. Borowiec, M.L., Lee, E.K., Chiu, J.C., and Plachetzki, D.C. (2015). Extracting phylogenetic signal and accounting for bias in whole-genome data sets supports the Ctenophora as sister to remaining Metazoa. BMC Genomics *16*, 987. 10.1186/s12864-015-2146-4.

118. Whelan, N.V., Kocot, K.M., Moroz, T.P., Mukherjee, K., Williams, P., Paulay, G., Moroz, L.L., and Halanych, K.M. (2017). Ctenophore relationships and their placement as the sister group to all other animals. Nat Ecol Evol *1*, 1737-1746. 10.1038/s41559-017-0331-3.

119. Laumer, C.E., Fernandez, R., Lemer, S., Combosch, D., Kocot, K.M., Riesgo, A., Andrade, S.C.S., Sterrer, W., Sorensen, M.V., and Giribet, G. (2019). Revisiting metazoan phylogeny with genomic sampling of all phyla. Proc Biol Sci *286*, 20190831. 10.1098/rspb.2019.0831.

120. Dellaporta, S.L., Xu, A., Sagasser, S., Jakob, W., Moreno, M.A., Buss, L.W., and Schierwater, B. (2006). Mitochondrial genome of Trichoplax adhaerens supports placozoa as the basal lower metazoan phylum. Proceedings of the National Academy of Sciences of the United States of America *103*, 8751-8756. 10.1073/pnas.0602076103.

**Graphical abstract**

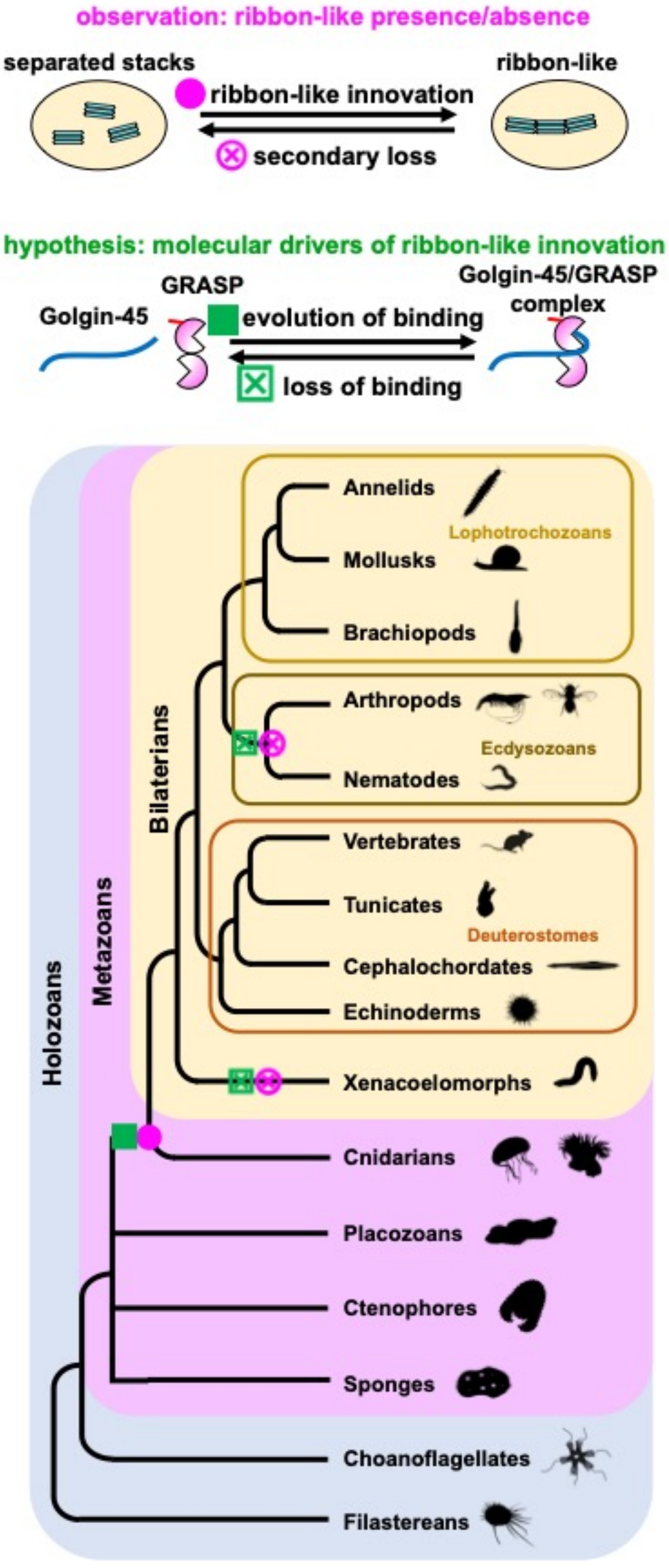

Figure 1

A

Multiple Golgi stacks per cell

Dispersed Golgi

Centralized (ribbon-like) Golgi

*Symsagittifera roscoffensis* (Xenacoelomorph)

B

*Calloria inconspicua* (Brachiopod)

C

*Platynereis dumerilii* (Annelid)

D

*Parhyale hawaiensis* (Arthropod)

E

*Clytia hemisphaerica* (Cnidarian)

F

*Mnemiopsis leidyi* (Ctenophore)

G

*Trichoplax adhaerens* (Placozoan)

H

*Oscarella carmela* (Sponge)

I

*Capsaspora owczarzaki* (Filasterean)

J

K

separated stacks

ribbon-like innovation

secondary loss

ribbon-like

Holozoans

Metazoans

Bilaterians

Filastereans

Choanoflagellates

Sponges

Ctenophores

Placozoans

Cnidarians

Xenacoelomorphs

Echinoderms

Cephalochordates

Tunicates

Vertebrates

Nematodes

Arthropods

Brachiopods

Mollusks

Annelids

literature

this report

# Figure 2

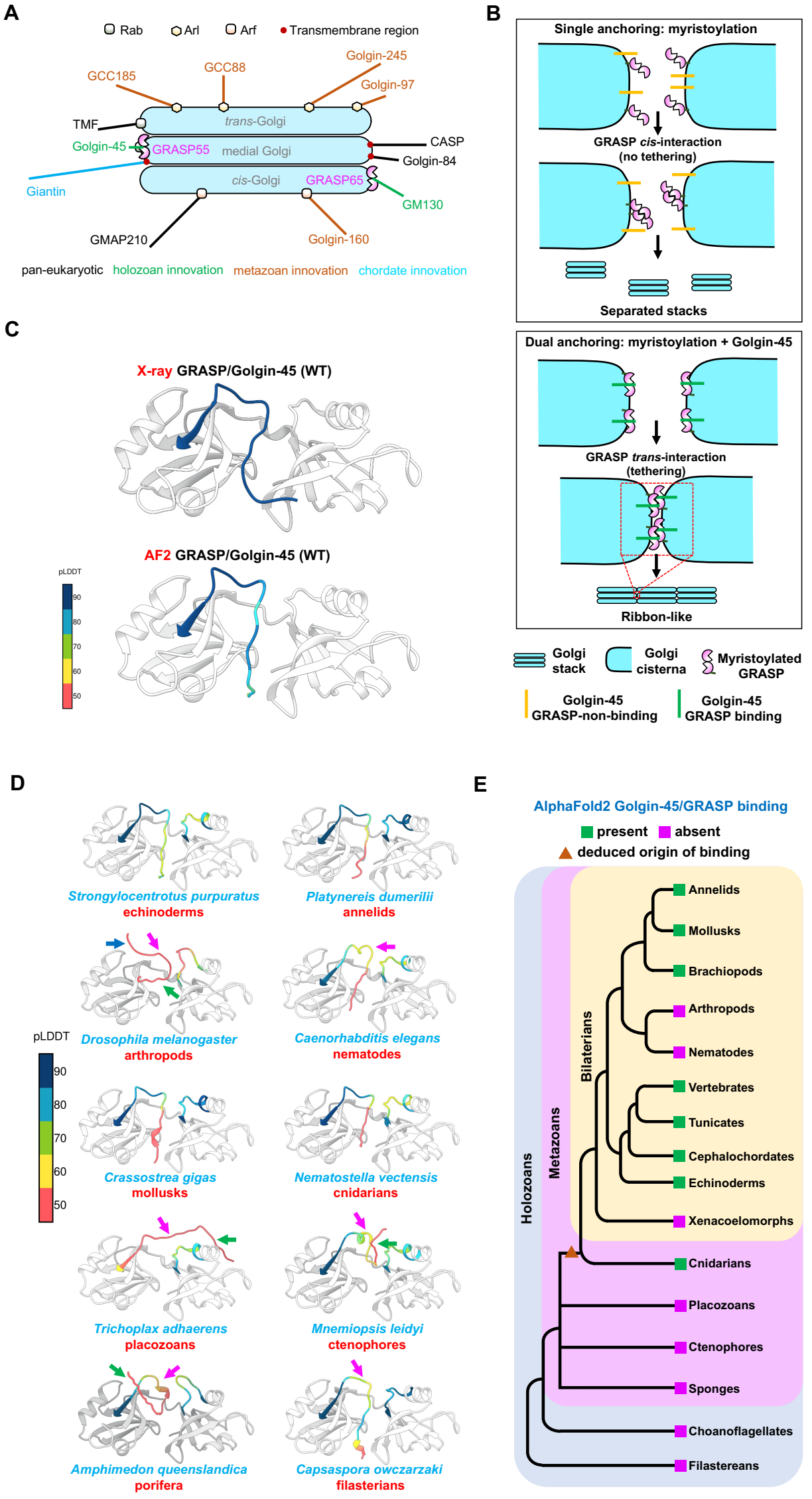
A
Rab
Arl
Arf
Transmembrane region
GCC185
GCC88
Golgin-245
Golgin-97
TMF
trans-Golgi
Golgin-45
GRASP55
medial Golgi
CASP
Golgin-84
Giantin
cis-Golgi
GRASP65
GM130
GMAP210
Golgin-160
pan-eukaryotic
holozoan innovation
metazoan innovation
chordate innovation
B
Single anchoring: myristoylation
GRASP cis-interaction
(no tethering)
Separated stacks
Dual anchoring: myristoylation + Golgin-45
GRASP trans-interaction
(tethering)
Ribbon-like
Golgi stack
Golgi cisterna
Myristoylated GRASP
Golgin-45 GRASP-non-binding
Golgin-45 GRASP binding
C
X-ray GRASP/Golgin-45 (WT)
AF2 GRASP/Golgin-45 (WT)
pLDDT
90
80
70
60
50
D
Strongylocentrotus purpuratus
echinoderms
Platynereis dumerilii
annelids
Drosophila melanogaster
arthropods
Caenorhabditis elegans
nematodes
Crassostrea gigas
mollusks
Nematostella vectensis
cnidarians
Trichoplax adhaerens
placozoans
Mnemiopsis leidyi
ctenophores
Amphimedon queenslandica
porifera
Capsaspora owczarzaki
filasterians
E
AlphaFold2 Golgin-45/GRASP binding
present
absent
deduced origin of binding
Holozoans
Metazoans
Bilaterians
Annelids
Mollusks
Brachiopods
Arthropods
Nematodes
Vertebrates
Tunicates
Cephalochordates
Echinoderms
Xenacoelomorphs
Cnidarians
Placozoans
Ctenophores
Sponges
Choanoflagellates
Filastereans

Figure 3

A

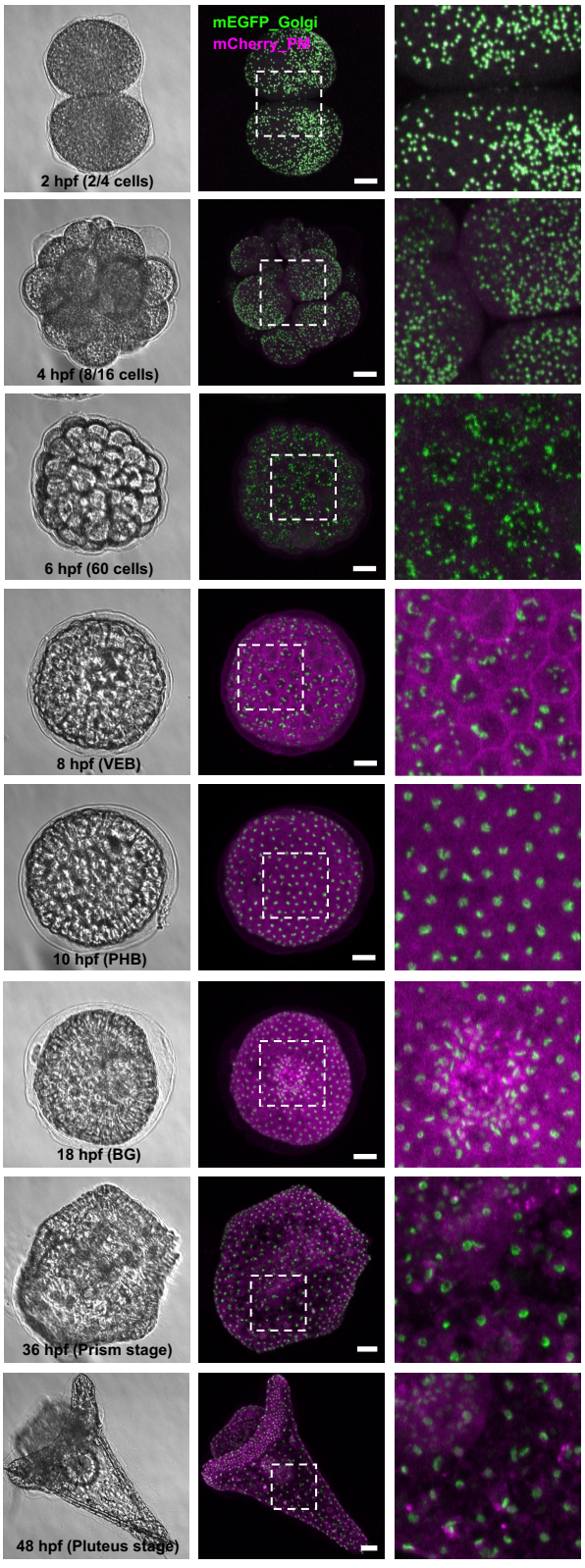


B

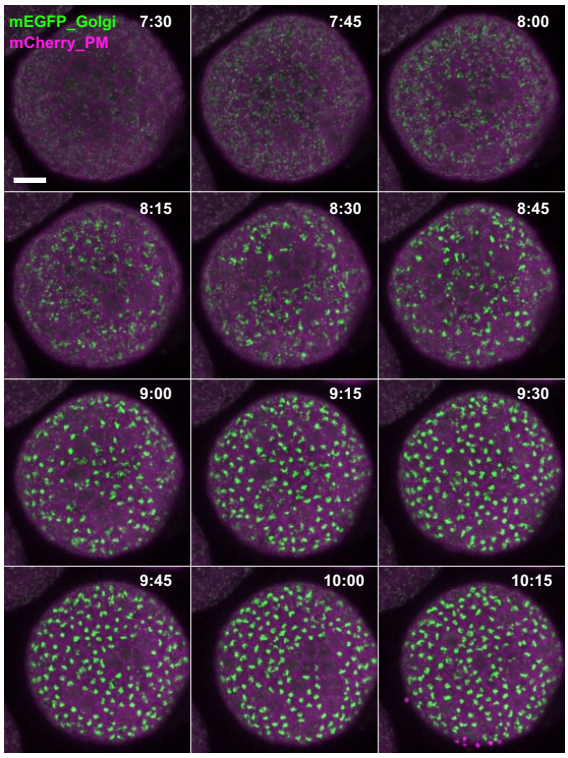


C

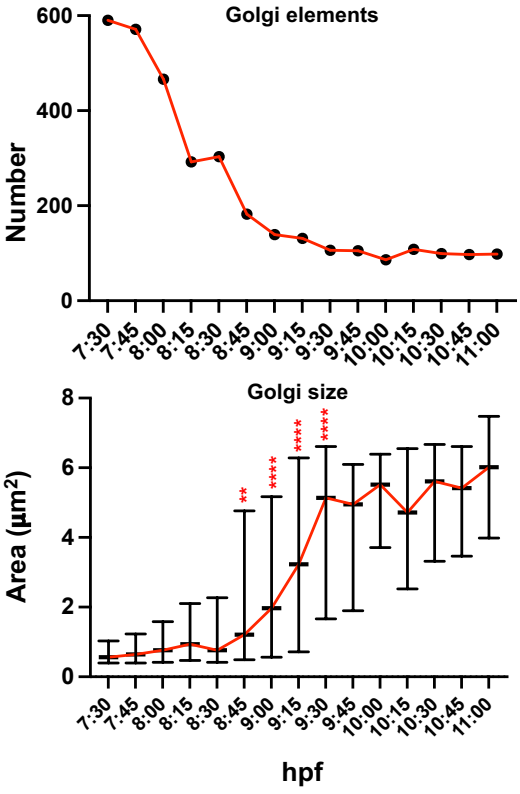


D

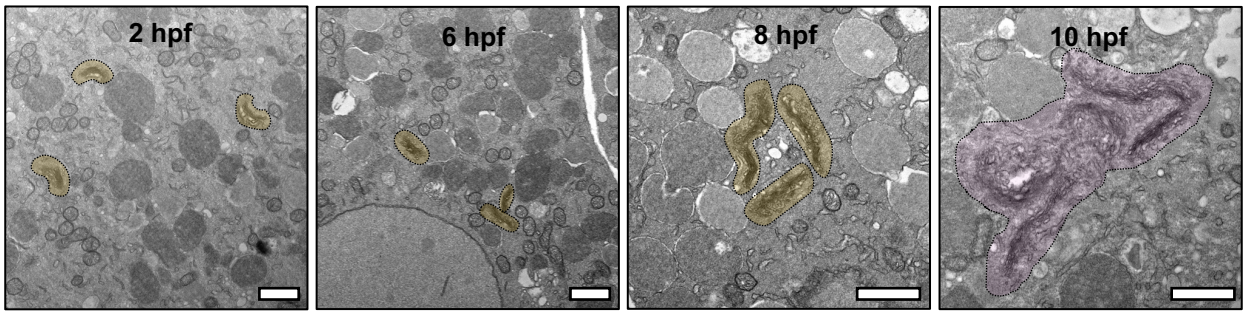


E

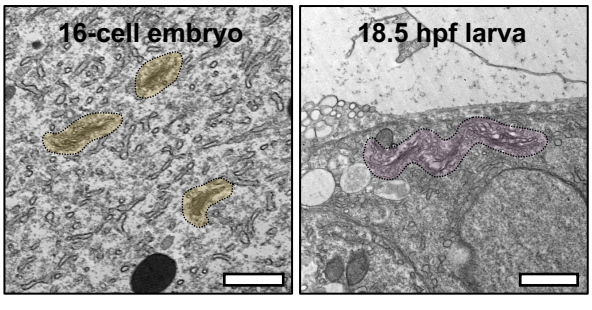

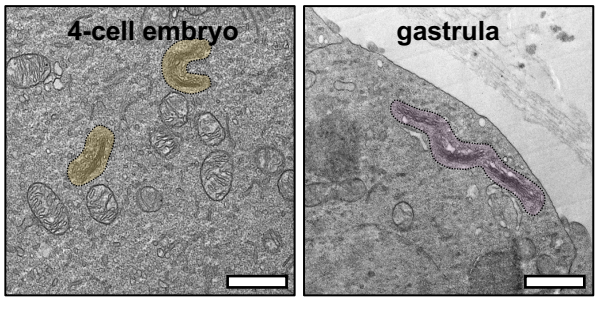
F